Available online at www.sciencedirect.com

SciVerse ScienceDirect

Geochimica et Cosmochimica Acta 85 (2012) 377–382

Geochimica et Cosmochimica Acta

www.elsevier.com/locate/gca

Response

Response to the Comment by S.B. Simon, L. Grossman, and S.R. Sutton on "Valence state of titanium in the Wark-Lovering rim of a Leoville CAI as a record of progressive oxidation in the early Solar Nebula"

Edward D. Young [a], Kathryn A. Dyl [b,*], Justin I. Simon [c]

[a] Department of Earth and Space Sciences, University of California Los Angeles, 3806 Geology Building, 595 Charles E. Young Drive East, Los Angeles, CA 90095-1567, USA

[b] Department of Earth Sciences and Engineering, Imperial College, London SW7 2AZ, UK

[c] Center for Isotope Cosmochemistry and Geochronology, ARES, NASA Johnson Space Center, Houston, TX 77058, USA

Available online 15 February 2012

Abstract

S. Simon et al. incorrectly suggest that in earlier work we claimed there was no Ti^{3+} in Wark-Lovering rim pyroxenes. In neither the paper by Simon et al. (2005) nor the subsequent paper by Dyl et al. (2011) did we assert that there was no Ti^{3+} in rim pyroxenes. Rather, we found that many pyroxenes have Ti^{3+} below detection while others have lower Ti^{3+}/Ti^{4+} than is typical of CAI interiors, indicating rim formation in a relatively oxidizing environment. Dyl et al. (2011) showed through exhaustive testing that the suggestion by Simon et al. (2007) that EMPA data in the paper by Simon et al. (2005) were flawed is incorrect. Here we consider each point raised in the comment by S. Simon et al. and reiterate that our electron microprobe data and the XANES data of Simon et al. (2007) agree and demonstrate a statistically significant ($\sim 2\sigma$) or greater difference between rim and interior pyroxene Ti^{3+}/Ti^{4+}. We show that the oxidation states of Ti in Wark-Lovering rim pyroxenes, the chemistry of rim pyroxenes, and the modal abundances of rim minerals are best explained by reaction between the CAI and gas that was orders of magnitude more oxidizing than the solar-like gas from which the CAIs originally formed.

1. INTRODUCTION

The fundamental conclusion of the work by Dyl et al. (2011) and the earlier study by Simon et al. (2005) was not that Wark-Lovering(WL) rims have absolutely no Ti^{3+}, as suggested by S. Simon et al., but rather that the Ti^{3+}/Ti^{4+} ratios of rim pyroxene record oxidizing conditions compared with those attending CAI formation. S. Simon et al. evidently disagree with the conclusion that there is lower Ti^{3+}/Ti^{4+} in rim pyroxenes compared with pyroxenes in the interiors of CAIs, and they suggest there is no evidence in rims for oxidation. We reiterate that oxidation during WL rim formation is supported not only by measured Ti^{3+}/Ti^{4+}but also by thermodynamic calculations depicting the chemical potential driving forces that give rise to the observed minerals comprising the rims (Simon et al., 2005) and a detailed analysis of the reaction space traversed during rim growth (Dyl et al., 2011). We welcome the opportunity to clarify our findings.

2. PYROXENE CHEMISTRY AND VERACITY OF EMPA ANALYSES

Dyl et al. (2011) set out to test the proposal by Simon et al. (2007) that the electron microprobe analyzer (EMPA) data presented in Simon et al. (2005) are spurious due to mixing of characteristic X-rays from spinel with X-rays from target pyroxenes. Simon et al. (2007) suggested that WL rim pyroxene analyses reported by Simon et al.

* Corresponding author.
E-mail addresses: kdyl@imperial.ac.uk, katie.dyl@gmail.com (K.A. Dyl).

0016-7037/$ - see front matter © 2012 Elsevier Ltd. All rights reserved.
http://dx.doi.org/10.1016/j.gca.2012.01.029

(2005) and Dyl et al. (2011) are corrupted by nearby spinels, a point these authors restate in their comment. Dyl et al. took the suggestion seriously and tested it experimentally. They performed analyses across pyroxene-spinel boundaries and found that this effect occurs within <1.5 μm from the boundary between the phases, but is absent beyond this distance from the inter-mineral boundary. All pyroxene analyses reported by Dyl et al. and J. Simon et al. are from spots very much greater than several μm distant from the closest spinel grain. What is more, Dyl et al. compared the data in question to theoretical and measured spinel-pyroxene mixing trends (the two agree) in a variety of bivariate plots representing composition space. Contamination by spinel should show up for all of the elements involved, and so these plots presented by Dyl et al. provide a rigorous test of the suggestion by S. Simon et al. The results (Figs. 3–7, Dyl et al., 2011) show that trends of spinel–pyroxene mixing do not overlap WL rim pyroxene data in composition space defined in terms of Ca, Si, Mg, and Ti. In some instances the data are in fact orthogonal to the spinel-pyroxene mixing trends (e.g., Fig. 4 in Dyl et al., 2011). In addition, an untenably large fraction of the pyroxene analyses would have to be dominated by spinel, over 15%, in order to explain the reduction in Ti^{3+} and Ca per formula unit observed in rim pyroxenes (e.g., Fig. 3 in Dyl et al., 2011).

In spite of this exhaustive testing, S. Simon et al. in their comment continue to assert that the rim pyroxene EMPA analyses are polluted by spinel. They posit that crude correlations between the number of cations per six oxygens with Al and Ca cation abundances in some pyroxenes cannot be explained by random analytical error. On this last point, we agree, but we did not suggest that random errors were to blame. Rather, Dyl et al. (2011) and Simon et al. (2005) showed these correlations to be the result of the variations in pyroxene chemistry (including oxidation state) arising from WL rim growth.

For example, Fig. 11 of Dyl et al. (2011) shows that as Ca is replaced by Mg in the pyroxene M2 site, represented by an increase in the $Mg_2Si_2O_6$ (enstatite, en) component in rim pyroxene, the number of cations per 6 oxygens will increase when calculated on the basis of total $Ti = Ti^{4+}$ precisely because Ti^{3+} is replaced by Ti^{4+} in the pyroxene substitution mechanism. The same analysis demonstrates that the $CaAl_2SiO_6$ (Ca-tschermak, CATs) component in the pyroxene rises at the expense of the $CaMgSi_2O_6$ (diopside, di) component simultaneously (for the complete analysis, see Dyl et al. (2011)). The result is a positive correlation between total cations (calculated using $Ti = Ti^{4+}$) and Al and a negative correlation between Ca and Al, as observed. Simon et al. (2007, and this comment) attribute these trends to analytical artifacts whereas Dyl et al. (2011) show that they are expected from the mechanism for WL growth.

We note that part of the concern expressed by S. Simon et al. arises from the assertion that no pyroxenes should have less than 1.0 Ca cation per 6-oxygen formula unit (Simon et al., 2007). We regard this assertion as wholly inconsistent with what is known about the crystal chemistry of pyroxenes in rocks of all kinds and see no reasons why WL rims should be immune from the effects of whole-rock reactions on the M2 site occupancy in pyroxenes that are so evident in other rocks. Dyl et al. (2011) quantified the effects of reactions that formed WL rims on pyroxene M2 site occupancy with the reaction space analysis of WL rim formation.

3. SAMPLING AND DATA DISTRIBUTION

3.1. Titanium concentrations of rim pyroxenes

S. Simon et al. suggest that the paper by Dyl et al. (2011) is misleading because in the original data set from Simon et al. (2005), there was very little or no Ti^{3+} in most spots analyzed. S. Simon et al. characterize these results as showing that "…Ti^{3+}/Ti^{4+} ratios of rim pyroxene are generally *slightly* [italics added] lower than those of interior pyroxene, but not to the extent that Ti^{3+} is absent from the rims…". Dyl et al. used a probability density plot (Fig. 8, Dyl et al., 2011, reproduced as Fig. 1 in this reply) precisely to avoid such qualitative descriptions of the data, relying instead on the distribution of data taking into account analytical uncertainties. The relative probability plot clearly shows a distinction between the rim and interior pyroxene Ti^{3+}/Ti^{4+}at the $\sim 2\sigma$ level. The distinction may be even greater if it turns out that the lower Ti pyroxenes analyzed by Simon et al. (2005)

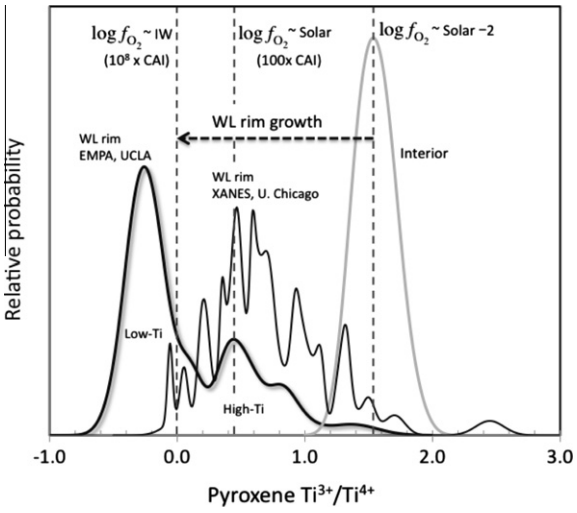

Fig. 1. Probability density plot reproduced from Dyl et al. (2011) annotated to show correspondence between measured pyroxene Ti^{3+}/Ti^{4+} and calculated oxygen fugacity ($\log f_{O_2}$) following the method of Simon et al. (2005). The bold black curve is the probability distribution for the WL rim data from Simon et al. (2005) and Dyl et al. (2011). The thinner black curve shows the WL rim XANES data from Simon et al. (2007). The grey curve is composed of the data for the interior of CAI 144A from Simon et al. (2005). The high-Ti (Dyl et al., 2011) and low-Ti (Simon et al., 2005) EMPA data are indicated. The peak in the XANES and high-Ti EMPA data record oxygen fugacities 100× that of the CAI interior. The low-Ti pyroxenes record oxygen fugacities $10^8\times$ greater than the CAI interior.

are more abundant than the higher Ti pyroxenes in WL rims analyzed by Dyl et al. (2007) as is our impression (the precise relative amounts of pyroxenes of different compositions is yet to be quantified and is not well reflected in the data collected thus far).

Dyl et al. found more Ti^{3+} in the rim pyroxenes than did Simon et al. (2005), but we emphasize that this was by design. In the work presented by Simon et al. (2005) the focus was on pyroxenes with relatively low Ti concentrations (although still high for pyroxenes in general) that turned out to have virtually no detectable Ti^{3+}. These pyroxenes were targeted because they were abundant, showed the greatest departures in overall chemistry from the interior pyroxenes, and appear to be characteristic of the diopside layer of the WL rims. The point of the study by Dyl et al., as a response to the paper by Simon et al. (2007), was to analyze more spots in the WL rims with greater Ti concentrations that more closely match those samples targeted by X-ray absorption near edge structure (XANES). A direct comparison between EMPA and XANES data is not strictly achievable, however, because the XANES technique by its nature samples greater volumes than EMPA, and these large sampling regions (ca. 10 μm depth) are likely to represent averages of several distinct pyroxene compositions (the scale of variability in pyroxene composition is often less than 10 μm). The retargeting of our EMPA studies necessarily led to an increase in the number of pyroxene analyses that more closely resemble pyroxenes in the interior of the CAIs.

Dyl et al. also added another CAI (Ef3) in order to test whether more oxidizing conditions are recorded in rims other than in CAI 144A. They found that the WL rim of the second CAI also exhibited lower Ti^{3+}/Ti^{4+} than interiors. Results based on the expanded data set of Dyl et al. demonstrate that pyroxenes in WL rims record a *progression* from $\log f_{O_2} \sim \text{solar} - 2$ to oxygen fugacities closer to those typical of planet formation (e.g., within a couple of log units of the iron-wüstite, IW, buffer).

3.2. Negative Ti^{3+} values

Negative Ti^{3+} abundances in Ti-poor rim pyroxene analyses presented by Simon et al. (2005) are mentioned by S. Simon et al. as a source of bias in the presentation of rim pyroxene EMPA data. However, as explained below, negative calculated Ti^{3+} per formula unit are to be expected for titanian pyroxenes with little or no Ti^{3+}. Consideration of the source of the negative Ti^{3+} estimates indicates that the negative values do not alter the conclusion that rim pyroxenes are appreciably lower in Ti^{3+}/Ti^{4+} than CAI interiors. Simon et al. (2005) attributed these negative values to accumulation of analytical errors that are necessarily accommodated by variable Ti valence. Pyroxenes, unlike some other silicates, are amenable to estimating valence states of constituent cations by EMPA analysis because of the lack of cation vacancies, allowing for the assumption of charge balance subject to the limitations of the precision of the analyses. Accordingly, we estimate Ti^{3+} per formula unit (pfu) from the expression

$$Ti^{3+}\text{pfu} = 2(n_O^{\text{cation norm}} - n_O^{\text{stoichiometric}}) \quad (1)$$

Where $n_O^{\text{cation norm}}$ is the number of oxygens calculated on the basis of 4.0 cations, total $Ti = Ti^{4+}$ and total $Fe = Fe^{2+}$, and total $Cr = Cr^{3+}$ (the assumed valence state for Cr is of negligible impact due to the low concentration of Cr) while $n_O^{\text{stoichiometric}}$ is the stoichiometric number of oxygens, in this case 6. An excess of calculated oxygens per cation-normalized formula unit reflects an excess in positive charge. Conversely, a deficit in positive charge will result in a paucity of oxygens in cation-normalized formulae, resulting in negative Ti^{3+}pfu using Eq. (1). Cation charge deficiencies appear as excess cations relative to stoichiometric in formulae normalized to six oxygens. Negative Ti^{3+}pfu, like those observed, can therefore arise from analytical errors that result in cation totals exceeding the stoichiometric value of 4.00 per six oxygens by 0.5% or less (e.g. 4.01–4.02 vs. 4.00, Table 2 of Simon et al., 2005). Accumulated analytical errors on the order of 0.5% in cation totals can cause negative Ti^{3+}pfu where Ti^{3+} is essentially absent, as discussed by Simon et al. (2005).

Alternatively, negative calculated Ti^{3+}pfu could signify non-negligible concentrations of cations other than Ti with valence states differing from those assumed. The most likely candidate is ferric iron. The expression for estimating ferric iron from charge balance is

$$Fe^{3+}\text{pfu} = -2(n_O^{\text{cation norm}} - n_O^{\text{stoichiometric}}). \quad (2)$$

Comparing Eqs. (1) and (2) shows that unrecognized Fe^{3+} will appear as negative Ti^{3+}pfu. Oxygen fugacities where Ti^{3+} and Ti^{4+} coexist do not overlap appreciably with oxygen fugacities where Fe^{2+} and Fe^{3+} coexist (similar arguments obtain for Cr^{2+} and Cr^{3+}) (Papike et al., 2005). As a result, where Ti exists in both 3^+ and 4^+ states, as in CAI interiors, it is generally not necessary to consider multiple valence states for other cations like Fe and Cr, vanadium being a notable exception (although V concentrations are sufficiently low as to be of limited importance in this context). However, at higher oxygen fugacities where Ti^{3+} is absent, the oxidation state of Fe can be variable and can cause negative calculated Ti^{3+}pfu.

For example, we tested our algorithm for estimating the valence state of Ti on terrestrial and lunar titanianaugite EMPA analyses reported by Tracy and Robinson (1977). We obtain Ti^{3+}/Ti^{4+} values that agree with the results of that study for lunar pyroxenes where all Fe occurs as Fe^{2+} due to the reducing conditions (IW-2). Applying the Ti oxidation state algorithm to terrestrial pyroxenes that Tracy and Robinson calculate to have significant Fe^{3+} (where the authors assume no Ti^{3+} due to the more oxidizing conditions of formation) one derives negative Ti^{3+}pfu equivalent to the number of Fe^{3+}cations pfu calculated by Tracy and Robinson. In other words, ignoring the presence of Fe^{3+} causes spurious assignment of the cation charge deficiency to negative Ti^{3+}. The salient point is that there is nothing wrong with these pyroxene analyses. Rather, the problem is a focus on variable oxidation states of Ti

when conditions are sufficiently oxidizing that iron has the variable oxidation states and not Ti. In the work by Dyl et al. and by J. Simon et al. variable oxidation states of iron were not considered. The occurrence of some Fe^{3+} in the most oxidized rim pyroxenes (low-Ti pyroxenes) cannot be ruled out because once Ti^{3+} is absent we do not have an upper limit on oxygen fugacity. In this case, such negative values would be another indicator of relatively oxidized rims.

The mere presence of negative Ti^{3+} values in low-Ti rim pyroxenes does not detract from the fact that rim pyroxenes are significantly lower in Ti^{3+}/Ti^{4+} than CAI interior pyroxenes. In order for negative Ti^{3+} values to be sufficient to make rim pyroxenes the same in Ti^{3+}/Ti^{4+} as CAI interior pyroxenes, the analyses would have to be plagued by unrealistically large and systematic errors or unrealistically high concentrations of Fe^{3+}.

3.3. Distribution of oxidation states of titanium

As shown in Dyl et al. (2011, Fig. 8), the result of the new targeting strategy for sampling rim pyroxenes was a data set in complete agreement with the XANES results of Simon et al. (2007) (Fig. 1). Importantly, Dyl et al. noted that both the EMPA and XANES data sets for CAI Leoville 144A show markedly lower Ti^{3+}/Ti^{4+}in WL rims than in the interior of the CAI, even for the highest Ti concentrations, with rims by EMPA showing distribution peaks at 0 (calculated values down to −0.5, see above) and 0.45 and rims by XANES showing a broader peak at ~0.5. These results are to be compared with interiors showing a relatively sharp peak at 1.5 (Dyl et al., 2011, Fig. 8). For reasons that evade us, Simon et al. (2007) interpreted their XANES results showing lower pyroxene Ti^{3+}/Ti^{4+}than in the interiors as being indicative of no difference in oxidation state between the two parts of the CAI. We pointed out here that while they concluded the rims are not more oxidized than the interiors, their data imply otherwise.

We do not disagree with most of the characterization of the data as presented in paragraph 2 of §2.1 in the comment by S. Simon et al. However, S. Simon et al. in their comment present a histogram displaying their XANES data for WL rims and EMPA data for CAI interiors that apparently excludes all of the EMPA data reported by Simon et al. (2005) and Dyl et al. (2011). The difference between their distribution of data and that shown in Fig. 8 of Dyl et al. (2011) is mainly in the spread in the data for the CAI interiors (the reader may convert $R = Ti^{3+}/Ti^{4+}$ in Fig. 1 to $x = Ti^{3+}/(Ti^{4+}+Ti^{3+})$ shown in Fig. 1 of the S. Simon et al. comment with the relation $x = R/(R+1)$). Results for the CAI interior reported by J. Simon et al. and Dyl et al. cluster considerably more tightly than the data for interiors shown by S. Simon et al. As the CAI that was the focus of the former two studies was relatively pristine, we have confidence that the tight clustering showing $Ti^{3+}/Ti^{4+} \sim 1.5 \pm 0.5$ (2σ) is characteristic of the unaltered CAI interior. The distinction between rim and interior pyroxene oxidation states is statistically significant (Fig. 1; Dyl et al., 2011). We have not seen evidence with our calculation and analytical EMPA methods that unaltered pyroxenes in CAI interiors have $Ti^{3+}/Ti^{4+} < 0.5$ (corresponding to $Ti^{3+}/Ti_{total} < 0.33$), as indicated in the Figure by S. Simon et al.

In addition to the larger spread in oxidation states in the interior pyroxenes, rim pyroxene data in the histogram by S. Simon et al. include rims that are petrographically rather different from that of CAI 144A (compare Fig. 1 of Dyl et al. 2011 to Fig. 6 of Simon et al. (2007); discussion in Dyl et al. (2011)). These rims exhibit less distinct boundaries between spinel layers and pyroxene layers, resulting in a diffuse gradation from interior to rim-like pyroxene compositions as the outer edge of the rim is approached. We note that the relatively constant and high Ti^{3+}/Ti^{4+} for rim pyroxenes in CAI 144A shown in Fig. 12 of Simon et al. (2007) is misleading as it represents only a fraction of the XANES data in their data table. Our probability density plot (Fig. 1, after Dyl et al. (2011)) includes all of the XANES data published by S. Simon et al.

We can only speculate as to the origin of the larger spread in the Ti^{3+}/Ti^{4+} data shown by S. Simon et al. One possibility is the large data set includes a commensurately large variation in petrographic occurrences that will require more detailed investigation. Another is that their data processing and/or analytical methods differ from our own. In any case, we stand by the data distribution shown in Fig. 1 as being indicative of relatively oxidizing conditions during rim formation.

4. CALCULATION OF OXYGEN FUGACITIES

S. Simon et al. suggest that conversion of Ti^{3+}/Ti^{4+}values to oxygen fugacities is premature in view of uncertainties in both the temperature of formation of the rims and ratios of partial pressures of SiO and Mg (P_{SiO}/P_{Mg}) during rim formation. Although application of equilibrium thermodynamics is always questionable in low-pressure systems such as the early solar protoplanetary gas disk, we do not agree that calculated oxygen fugacities are compromised by uncertainties in temperature and $P_{SiO}/P_{Mg}$for the reasons discussed below.

4.1. Partial pressures of SiO and Mg

Differences in f_{O_2} arising from differences in rim and interior pyroxene Ti^{3+}/Ti^{4+}calculated using Eq. (7) in Simon et al. (2005) are insensitive to the partial pressure ratio of SiO and Mg given that the differences in oxygen fugacity are on the scale of many orders of magnitude. This is because from Eq. (7) in that work

$$\frac{\partial \Delta \log f_{O_2}}{\partial \Delta \log(P_{SiO}/P_{Mg})} = 2, \quad (3)$$

meaning that changes in $\log(P_{SiO}/P_{Mg})$ would have to be similar in magnitude to changes in $\log f_{O_2}$ if the latter was due solely to the former. J. Simon et al. pointed out that SiO and Mg behave similarly due to similarities in the volatilities of silicon and magnesium in condensed phases, and separating their partial pressures by orders of magnitude is

not consistent with what is known about the chemistry of these elements at conditions that apply to the early solar system (e.g., Richter et al., 2002). We stand by our original conclusion for these reasons.

4.2. Effects of temperature

S. Simon et al. suggest in their comment that a difference in the temperature between formation of the CAI interior and the rim alone might explain the differences in activities of Ti^{3+} and Ti^{4+} we observe (not withstanding their assertion that there is no such difference) with no appreciable change in oxygen fugacity. Here we explain the implications of this suggestion using Fig. 2 modified from Fig. 4 of Simon et al. (2005). Contours of the logarithm of the ratio of the activities of the $CaTi^{4+}Al_2O_6$ and $CaTi^{3+}AlSiO_6$ end-member pyroxene components in CAI 144A show that a difference of 150° at constant oxygen fugacity would be required to explain the shift from the pyroxene Ti^{3+}/Ti^{4+} of the CAI interior to the modes in the rim XANES data (Simon et al., 2007) and the high-Ti rim pyroxene EMPA data (Dyl et al., 2011). The low-Ti pyroxenes with virtually no detectable Ti^{3+} (e.g., Simon et al., 2005) would require the rims to form ~600 degrees or more lower than the CAI interiors if oxygen fugacity did not increase (Fig. 2). Formation of rims at such low temperatures (near 1100 K based on the solidus of CAIs) is difficult to envision, although we cannot rule it out categorically.

More importantly, the mechanism that would impose a fixed oxygen fugacity on the system during such large changes in temperature is not clear given that at the required low temperatures these f_{O_2} values would be greater than solar values by six orders of magnitude. The difficulty is that it is extremely rare, if not virtually impossible, to change temperature in a chemical system involving oxygen and other gas species without changing f_{O_2} as well. Indeed one would have to devise an extraordinary contrivance in the laboratory to conduct an experiment over a wide range of temperature but fixed oxygen fugacity. Such an experiment would require a flux of gas of continually varying composition to offset the effects of temperature, for example. Many natural systems may not be rigorously buffered (where a fixed f_{O_2} is impossible with changing T), but they are typically pseudo-buffered because there is a trade off between speciation and temperature. The agent that held f_{O_2} to low values characteristic of CAI formation was a hydrogen-rich solar-like gas. A solar-like gas, rich in hydrogen, buffers f_{O_2} with temperature, as shown in Fig. 2. In the general case in a hydrogen-rich gas where sources of oxygen exist (e.g., evaporating ice or rock dust), varying temperature will not be accompanied by a fixed oxygen fugacity. Instead, f_{O_2} will exhibit a positive correlation with temperature by virtue of altering the H_2/H_2O ratio in the gas as shown in Fig. 2 (Krot et al., 2005). For these reasons we do not agree that differences in temperature at fixed oxygen fugacity is a viable

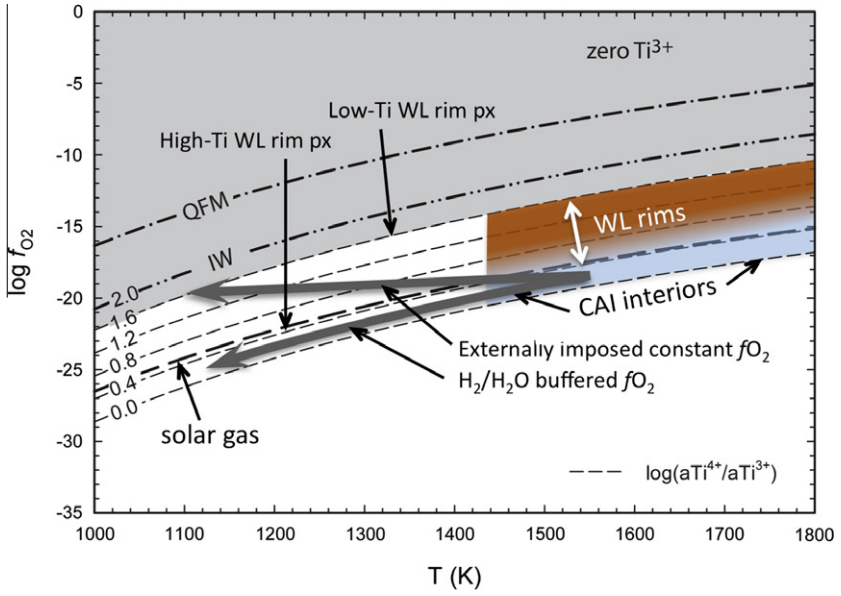

Fig. 2. Logf_{O_2} versus temperature based on thermodynamic calculations presented by Simon et al. (2005). Thin dashed contours show isopleths for the logarithms of ratios of activities of $CaTi^{4+}Al_2O_6$ and $CaTi^{3+}AlSiO_6$in CAI 144A pyroxenes based on Eq. (7) of Simon et al. (2005). The positions of CAI interior pyroxenes and ~ pyroxenes in WL rims are shown in blue and red, respectively, with a gradation in the latter reflecting the variation in WL pyroxene compositions. The activity ratio contour for the mode in the high-Ti WL rim pyroxene data from Dyl et al. (2011) and Simon et al. (2007) and the contour for the low-Ti WL rim pyroxenes are indicated. Region of no Ti^{3+} is shown in grey. Two illustrative paths for decreasing temperature that accommodate the range of Ti^{3+}/Ti^{4+} in CAI and WL rim pyroxenes are shown. One depicts changing temperature with an externally imposed f_{O_2} and the other changing temperature with f_{O_2} prescribed by H_2/H_2O buffering by a solar-like gas (see text). Also shown for reference are the quartz–magnetite_fayalite (QFM), iron–wüstite (IW) and solar gas buffer curves. Modified after Simon et al. (2005).

explanation for the shift in pyroxene Ti^{3+}/Ti^{4+} from CAI interiors to rims.

5. ROLE OF SECONDARY ALTERATION

S. Simon et al. dismiss arguments by Dyl et al. against aqueous alteration as an explanation for the higher oxidation state of WL rim pyroxenes relative to the CAI interiors. We are vexed by the coexistence of their argument that the rims are not demonstrably oxidized on the one hand, and their suggestion of an alternative explanation as to why they are oxidized on the other. In any event, accepting that the rims are oxidized, we found that the overall differences between CAI interiors and WL rims in both pyroxene chemistry and modal mineralogy can be explained quantitatively by reactions between the CAI and nebular gas, as described in detail by Dyl et al. (2011). S. Simon et al. offer no quantitative assessment of their suggestion that the oxidation is due to aqueous alteration. Until such time as a model for secondary aqueous alteration is put forward that successfully explains the mode and mineral chemistry of WL rims, we stand by our conclusion that the pyroxene chemistry of WL rims and CAI interiors is best explained by our proposed mechanism for WL rim formation.

S. Simon et al. point to greater Fe content of pyroxenes in WL rims as suggestive of aqueous alteration. This is not a unique interpretation. Iron concentrations in rim pyroxenes compared with interior pyroxenes are explained by more oxidizing conditions in general, consistent with our conclusion that rims formed in relatively dust rich, and therefore oxidizing, conditions in the solar nebula. An increase in the concentration of Fe (concurrent with an increase in the concentration of Mg) in rim pyroxene is a prediction of our model.

6. CONCLUSION

S. Simon et al. are correct that in our 2005 paper we concluded that f_{O_2} of rim formation was near IW-1. This was based on sampling the most oxidized of the pyroxenes. We note that no such pyroxenes are found in the interiors of the CAIs to our knowledge. Dyl et al. (2011) present an expanded data set suggesting that rims recorded a range of f_{O_2} up to $\sim$IW-1. The distinction, while real, is not important to the main conclusion of both papers: outboard of the hibonite/spinel layers, there is ample evidence that WL rims formed by mineral growth in response to large chemical potential gradients under conditions more oxidizing than the CAIs themselves. We stand by this conclusion. The high-Ti pyroxenes in the WL rims record $f_{O_2}\sim 100\times$ that of the CAI interior, and the low-Ti pyroxenes record $f_{O_2}\sim 8$ log units greater than that of the CAI interior.

S. Simon et al. do not address the critical point that not only do both data sets, our EMPA data and their rim XANES data, show that where the WL rim of the CAI is well defined it is more oxidized than the interior, but that this is exactly what is predicted when one uses the cation chemistry of the pyroxenes and modal abundances of rim minerals to reconstruct the mechanism of WL growth. We infer that our results for the two CAIs we have studied pertain to WL rim formation in general. This inference warrants further testing.

REFERENCES

Dyl K. A., Simon J. I. and Young E. D. (2011) Valence state of titanium in the Wark-Lovering rim of a Leoville CAI as a record of progressive oxidation in the early Solar Nebula. *Geochim. Cosmochim. Acta* **75**(3), 937–949.

Krot A. N., Hutcheon I. D., Yurimoto H., Cuzzi J. N., McKeegan K. D., Scott E. R. D., Libourel G., Chaussidon M., Aleon J. and Petaev M. I. (2005) Evolution of oxygen isotopic composition in the inner solar nebula. *Astrophys. J.* **622**, 1333–1342.

Papike J. J., Karner J. M. and Shearer C. K. (2005) Comparative planetary mineralogy: valence state partitioning of Cr, Fe, Ti and V among crystallographic sites in olivine, pyroxene, and spinel from planetary basalts. *Am. Mineral.* **90**, 277–290.

Richter F. M., Davis A. M., Ebel D. S. and Hashimoto A. (2002) Elemental and isotopic fractionation of type B calcium-aluminum-rich inclusions: experiments, theoretical considerations, and constraints on their thermal evolution. *Geochim. Cosmochim. Acta* **66**(3), 521–540.

Simon J. I., Young E. D., Russell S. S., Tonui E. K., Dyl K. A. and Manning C. E. (2005) A short timescale for changing oxygen fugacity in the solar nebula revealed by high-resolution ^{26}Al–^{26}Mg dating of CAI rims. *Earth Planet. Sci. Lett.* **238**(3–4), 272–283.

Simon S. S. B., Sutton S. R. and Grossman L. (2007) Valence of titanium and vanadium in pyroxene in refractory inclusion interiors and rims. *Geochim. Cosmochim. Acta* **71**, 3098–3118.

Tracy R. J. and Robinson P. (1977) Zoned titanian augite in alkali olivine basalt from Tahiti and the nature of titanium substitutions in augite. *Am. Mineral.* **62**, 634–645.

Associate editor: Alexander N. Krot